

Coreset Selection via LLM-based Concept Bottlenecks

Akshay Mehra^{1*}, Trisha Mittal^{1*}, Subhadra Gopalakrishnan², and Joshua Kimball¹

^{*}Equal Contribution ¹Dolby Laboratory ²Apple
 {akshay.mehra, trisha.mittal, joshua.kimball}@dolby.com

Abstract

Coreset Selection (CS) aims to identify a subset of the training dataset that achieves model performance comparable to using the entire dataset. Many state-of-the-art CS methods select coresets using scores whose computation requires training the downstream model on the entire dataset first and recording changes in the model’s behavior on samples as it trains (training dynamics). These scores are inefficient to compute and hard to interpret, as they do not indicate whether a sample is difficult to learn in general or only for a specific downstream model. Our work addresses these challenges by proposing a score that computes a sample’s difficulty using human-understandable textual attributes (concepts) independent of any downstream model. Specifically, we measure the alignment between a sample’s visual features and concept bottlenecks, derived via large language models, by training a linear concept bottleneck layer and computing the sample’s difficulty score using it. We then use stratified sampling based on this score to generate a coreset of the dataset. Crucially, our score is efficiently computable without training the downstream model on the full dataset even once, leads to high-performing coresets for various downstream models, and is computable even for an unlabeled dataset. Through experiments on CIFAR-10/100, and ImageNet-1K, we show that our coresets outperform random subsets, even at high pruning rates, and achieve model performance comparable to or better than coresets found by training dynamics-based methods.

1 Introduction

Machine learning (ML) pipelines are increasingly demanding more data and compute [70, 2] to achieve improved performance on various tasks. While in line with empirical neural scaling laws [28, 24, 22, 53] where a model’s performance improves with increasing model and training data size, these improvements come at an unsustainable cost of compute/energy. However, recently [65, 39] demonstrated that data pruning plays a crucial role in enabling an exponential reduction in test error with increasing dataset size, underscoring the importance of data quality over quantity.

Coreset Selection (CS) [44, 18, 50, 77, 43, 86, 10] is a data pruning technique that improves the efficiency of model training by pruning a large dataset and retaining only a small subset of representative samples. Most CS methods work by first using a score to estimate the difficulty/importance of every training sample and then using a sampling strategy that forms the coreset. Many state-of-the-art (SOTA) CS methods use the downstream model’s training dynamics — changes in the model’s behavior on a sample over epochs during training, to generate an importance score for each sample. While this enables a good estimation of the data importance, it requires training the downstream model on the entire dataset at least once, which can be costly when training a large model on a large dataset (see Fig. 1). While [11] showed that a coreset selected using

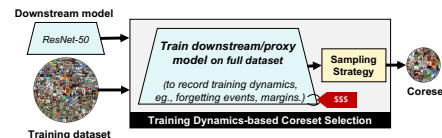


Figure 1: Computation of training dynamics-based scores require training the original or a big proxy model on the full dataset, to identify the coreset, making them computationally expensive.

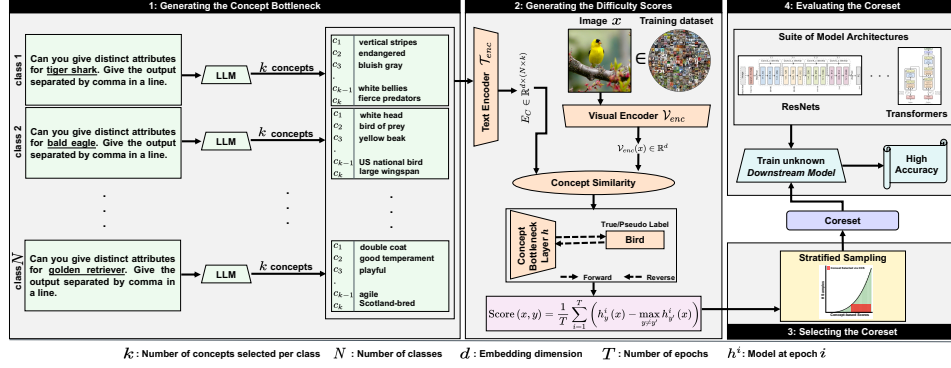


Figure 2: **Overview of our approach:** We start by prompting an LLM to generate concept annotation for N class label names in the dataset and select k most discriminative attributes (per class) to form the concept bottleneck, which are passed through a text encoder (T_{enc}) to obtain the bottleneck embedding matrix (E_C). The visual information of a training sample x extracted via the visual encoder (V_{enc}) is then aligned to E_C using a linear concept bottleneck layer (h) trained for T epochs. Our difficulty score for a sample x is then computed as the average margin (i.e., the difference between the likelihoods of the correct and other classes) over T epochs. Finally, the coreset is selected via stratified sampling and is used to train downstream models.

training dynamics of a mid-sized proxy model (eg, ResNet-18) is effective for a larger downstream model (eg, ResNet-50), training even such a model may not be feasible for large datasets. Moreover, since these scores are dependent on training dynamics of a particular downstream model, they are hard to interpret as they do not inform us about the sample’s importance for another downstream model (without training it first). Thus, in our work we tackle the following question: *“How to efficiently estimate the importance of training samples for CS, in a way that is independent of the downstream model and avoids training that model on the full dataset?”*

To address this, we use Concept Bottleneck Models (CBMs) [34, 83], which work by mapping a model’s input onto a set of human-understandable concepts, referred to as the “bottleneck” and use them to make a prediction. However, CBMs require concept annotation for every sample in the dataset, which can be costly to obtain. Recently [82, 79] showed that off-the-shelf Large Language Models (LLMs) and Vision Language Models (VLMs) can be prompted to obtain concept annotations for training samples without requiring any task-specific fine-tuning (see Fig. 2 (block 1)). Once the bottleneck is formed, we use a VLM (e.g., CLIP [52]) to measure the alignment between the visual features and the concept bottleneck (denoted as concept similarity in Fig. 2 (block 2)). A linear concept bottleneck layer is then trained to align the visual and concept features while classifying samples. We then use the average margin of a sample while training the bottleneck layer as our concept-based importance score. Finally, we form the coreset using stratified sampling [86] (block 3) based on our score, which can then be used for training downstream models (Fig. 2 (block 4)).

We empirically evaluate the effectiveness of our score on three benchmark datasets: CIFAR-10/100 [35] and Imagenet-1K [13]. Our results show that downstream models trained on our coresets consistently achieve better accuracy than randomly sampled subsets, especially at high data pruning rates, and achieve performance close to SOTA CS methods. We also show that our approach is effective for the label-free CS problem where the dataset is unlabeled and leads to models with superior performance compared to SOTA label-free CS methods, especially on Imagenet. Since our CS method is independent of the downstream model, we show that our coreset leads to high performance regardless of the architecture of the downstream model. Moreover, our method speeds up the computation of the coreset by ≈ 8 times compared to approaches based on the training dynamics of the downstream model. Lastly, we show that our concept-based difficulty score provides an intuitive explanation of why examples are easy/hard, independent of the downstream model. Our main contributions are summarized below:

- We propose a concept-based score that efficiently computes a training data sample’s importance for CS without training a downstream model on the full dataset, even once.
- Our coresets improve accuracy by $\approx 5\%$ over random subsets at high pruning rates, are competitive to SOTA methods, transfer to various architectures, and are computable without labels.

- We show that using CBMs with LLM-generated concepts makes our score interpretable, enabling a data-centric solution for identifying coresets.

2 Related Work

Coreset selection (CS). CS improves the efficiency of model training by selecting a subset of influential samples. Various approaches have been proposed to generate such a subset [18]. A popular approach uses influence functions [33, 8, 42, 58] which measures the influence of a sample by considering the effect of removing it from the model’s training. While effective, these approaches are computationally costly due to their dependence on higher-order derivatives. Approaches that use the dataset’s geometric properties such as are another popular choice for CS [60, 65, 16, 15, 26]. However, the high computational complexity due to their dependence on pairwise distances between the samples prohibits their use on large datasets. Another set of approaches select a subset by either matching the gradients to those computed on the entire dataset [44, 30] or use training dynamics of a model [68, 51, 38, 12, 50] to compute the importance of a sample. However, such approaches require repeated training of the downstream model to produce accurate importance scores. In comparison, our approach avoids using any knowledge of the downstream model for computing the difficulty scores. Unlike our work which focuses on data pruning, a different line of work [31, 71] improves the training efficiency by adaptively selecting the best subset of training data (see App. A).

Concept-based interpretability approaches. Concepts are defined as high-level semantics that refers to the abstract and human-interpretable meanings of the visual data, such as objects, actions, and scenes, as opposed to low-level features like edges or textures [76]. Concepts have been used in interpretable computer vision to bridge the gap between human understanding and machine perception in various tasks such as image classification. Such interpretability methods can be broadly classified as *post-hoc methods* (do not impose any model constraints) or *by-design* methods (see App. A). Concept Bottleneck Models (CBMs) extend interpretable-by-design approaches by using human-understandable attributes as an intermediate layer for predictions, as used in few-shot learning [36] and attribute learning [78, 55]. While interpretable, CBMs reliance on costly annotations and lower accuracy compared to end-to-end models limit their usage. Post-hoc Concept Bottleneck Models (PCBMs) address these issues by incorporating static knowledge bases (e.g., ConceptNet [66]) and residual connections to boost accuracy [83]. Recently [82, 79] incorporated LLMs to identify the concept bottleneck making classification more explainable. We build on this and use CBMs for CS.

3 Preliminaries

3.1 Coreset selection (CS) problem formulation

Consider a classification task and data distribution P . Let $\mathcal{D} = \{(x_i, y_i)\}_{i=1}^n$ denote the dataset of n training examples sampled i.i.d. from the distribution P where x_i denotes the data and $y_i \in \mathcal{Y}$ denotes the label from a set of N classes. CS [11, 86] aims to find a subset \mathcal{S} of \mathcal{D} consisting of $m \leq n$ samples such that the models trained on \mathcal{S} achieve performance comparable to models trained on \mathcal{D} . Let $\theta_{\mathcal{D}}$ and $\theta_{\mathcal{S}}$ denote the “downstream model” trained on \mathcal{D} and \mathcal{S} (coreset), respectively and ℓ be the loss function then the CS problem is as follows

$$\min_{\mathcal{S}: \mathcal{S} \subset \mathcal{D}, |\mathcal{S}|=m} \mathbb{E}_{(x,y) \sim P} [\ell(x, y | \theta_{\mathcal{S}})] - \mathbb{E}_{(x,y) \sim P} [\ell(x, y | \theta_{\mathcal{D}})]. \quad (1)$$

To find this subset \mathcal{S} , previous works have proposed scores that gauge a sample’s difficulty for a model. Approaches such as max entropy uncertainty sampling [38, 61], and least confidence [12] estimate difficulty using the uncertainty of the model’s predictions on a sample. Another set of approaches such as k -center greedy [60] uses geometric information of the data to filter out redundant samples. Yet, another set of approaches uses training dynamics of the downstream model to estimate the difficulty score. Scores such as the forgetting events [68] computed as the number of times a sample gets misclassified after being correctly classified earlier during model training, and the area under the margin (AUM) [51] which identifies mislabeled/difficult samples, fall in this category.

3.2 Concept bottleneck models (CBMs)

Recent advances in language model-guided CBMs utilize an off-the-shelf LLM to obtain concept bottlenecks which are then used to predict the labels. These works rely on pre-trained multi-modal

models (such as CLIP [52]) which consists of a visual encoder \mathcal{V}_{enc} and a text encoder \mathcal{T}_{enc} that can map images and text to a d -dimensional representation space. Let $C = \{c_1, c_2, \dots, c_{N_C}\}$ be the set of N_C concepts (bottleneck) generated via an LLM, we can then construct a bottleneck embedding matrix $E_C \in \mathbb{R}^{N_C \times d}$ such that each row of the matrix is mapping of the concept $c \in C$ after passing it through textual encoder \mathcal{T}_{enc} . Based on this, a CBM [82] produces a prediction $h(x) = f(g(\mathcal{V}_{enc}(x); E_C))$ for a sample x where $g : \mathbb{R}^d \rightarrow \mathbb{R}^{N_C}$ computes the similarity of the visual features to each concept in the bottleneck and $f : \mathbb{R}^{N_C} \rightarrow \Delta$ outputs the probability of each class in the label set \mathcal{Y} , where Δ is a N simplex. We discuss details of f and g in Sec. 4.

4 Methodology

4.1 Generating the concept bottleneck via off-the-shelf LLMs

Since obtaining data with concept annotation is costly, we use LLMs to generate concept annotation for the samples. However, generating attributes (word-level concepts) for all the samples in the dataset via LLMs is still costly, hence we generate word-level concepts *only* for class label names. This approach was recently shown to be effective at generating the concept bottleneck for interpretable image classification [79, 82]. In Figure 2 (block 1), we present the prompts provided to the LLMs to extract the concepts for various class label names. The responses of the LLM are then processed to remove formatting errors to obtain the concept sets. Once the per-class concepts are extracted, we select k discriminative concepts per class (concepts that are unique to a class) to form the concept bottleneck. Our final list of k concepts for a class contains its class name and $k - 1$ attributes generated by the LLM. Details of our prompt design, robustness check of different prompts, and examples of the generated attributes are mentioned in App. B.

4.2 Concept-based score for CS

We now describe how to use the concept bottleneck to produce a difficulty score for the samples in the dataset. We start by discussing how we learn the functions f and g described in Sec. 3.2 (see Fig. 2 (block 2)). We use the dot product between the visual embeddings of an image x i.e. $\mathcal{V}_{enc}(x)$ and the bottleneck embedding matrix E_C to measure the alignment between the visual and textual features [82, 79]. Concretely, we compute the concept similarity score for a sample x as

$$g(x; E_C) := \mathcal{V}_{enc}(x) \cdot E_C^\top. \quad (2)$$

To map the concept similarity score to a prediction in the label space \mathcal{Y} , we propose to use a linear (concept bottleneck layer) predictor denoted by f . Concretely, the function f with parameters $W \in \mathbb{R}^{N \times N_C}$ is given by $f(x; W) := g(x; E_C) \cdot W^\top$. We learn the parameters W using

$$W^* = \arg \min_W \frac{1}{n} \sum_{i=1}^n \ell(f(x_i; W), y_i), \quad (3)$$

where $\ell(f(x; W), y) = -\log(f(x; W)_y)$ is the cross-entropy loss. The output of the concept bottleneck layer is defined as, $h(x) := f(g(x; E_C); W^*)$. In practice, we learn W using mini-batch gradient descent by running the optimization for T epochs. We then compute the difficulty of each training sample using area under the margin (AUM) [51] while solving Eq. 3, quantifying the data difficulty as the margin of a training sample averaged over T training epochs. Concretely, margin of a sample (x, y) at an epoch t is $M^t(x, y) = h_y^t(x) - \max_{y' \neq y} h_{y'}^t(x)$, where $h_{y'}^t(x)$ is the prediction likelihood of the bottleneck layer at epoch t for a class y' . Thus, AUM (concept-based score) is

$$\text{AUM}(x, y) = \frac{1}{T} \sum_{t=1}^T M^t(x, y). \quad (4)$$

Recent works [51, 86, 87] have demonstrated the effectiveness of AUM for computing a sample’s difficulty for CS. However, [86, 87] compute AUM for a specific downstream model by training it on the entire dataset first, which is computationally costly. On the other hand, we integrate AUM with the training of a linear layer h , training which is significantly cheaper than training the downstream model (training h for 100 epochs takes only 7 minutes on Imagenet compared to 8 hours for training a ResNet-34 for 100 epochs). Moreover, since our score is independent of the downstream model, our coresets can be used for any downstream model without change, unlike training dynamics-based approaches that require computing their coresets again for different/new downstream models.

Sampling training examples to form a coreset. After obtaining data difficulty scores, a crucial step is choosing the samples to form the coreset. While many previous works [68, 11] have reported encouraging results keeping the most challenging samples (for our concept-based score this means samples with the smallest margin), recent works [86, 65] have shown that this could lead to a catastrophic drop in accuracies after training the downstream model on the coreset, especially when the size of the coreset is small. This is mainly due to poor sample coverage and potentially mislabeled data in the datasets. To remedy this, we use Coverage-centric Coreset Selection (CCS) proposed by [86] (see Alg. 1 in App. C.5) which filters out (potentially) mislabeled samples and uses a stratified sampling approach to form the coreset. This technique has been shown to consistently achieve superior results to the random baselines for various coreset sizes.

4.3 Concept-based score for label-free CS

Recently, there has been an interest [87, 43, 17] in identifying the representative samples from an unlabeled dataset so as to 1) reduce the samples that need to be labeled/annotated by humans and 2) improve the efficiency of model training by only training the model on a subset of data. Our concept-based score can also be effectively utilized for this task with a simple modification. Similar to previous works [43, 87, 65], we assume that we know the number of classes in the datasets. Additionally, we assume that we also know the names of the classes in the datasets. Previous works have demonstrated that VLMs such as CLIP [52] achieve excellent zero-shot performance without requiring fine-tuning on specific datasets. We leverage this capability of CLIP models to obtain pseudo-labels for our unlabeled dataset and use them to obtain our difficulty score as follows

$$\text{AUM}(x, y_{\text{pseudo}}) = \frac{1}{T} \sum_{t=1}^T M^t(x, y_{\text{pseudo}}), \quad (5)$$

where for an image x in the dataset $y_{\text{pseudo}} = \arg \max_{j \in \mathcal{Y}} \mathcal{V}_{\text{enc}}(x) \cdot \mathcal{W}_{\text{zeroshot}}^T$ where $\mathcal{W}_{\text{zeroshot}} \in \mathbb{R}^{N \times d}$ is a matrix with columns defined as $\mathcal{T}_{\text{enc}}(s_j)$ and $s_j = \text{"a photo of a } \{j^{\text{th}} \text{ class name}\}"$ for each class $j \in \mathcal{Y}$ [52, 75]. We use these scores along with CCS [86] to produce the coreset. Similar to [87, 43], the coreset is then assumed to be annotated by humans and models are trained on it.

5 Experiments

Datasets, models, and training: We focus on CS for classification tasks on three benchmark datasets namely, CIFAR-10, CIFAR-100 [35], and Imagenet-1K [13] datasets consisting of 50000, 50000, and 1.28 million samples spread across 10, 100, and 1000 classes, respectively. For CIFAR-10/CIFAR-100, we train a ResNet(RN)-18 as a downstream model and for Imagenet we train ResNet-18/34/50 [19], MobileNet [56], DenseNet [25], Wide ResNet [85], and ViT [14] as downstream models on the coresets. We use FFCV [37] to accelerate training on Imagenet. We run CS for three trials with different random seeds and report the average of these runs in our tables for various pruning rates where a pruning rate of 90% refers to removing 90% of the samples.

For generating concepts we use a recently proposed open source model LLaVA [41, 40]. For computing the concept similarity scores between the visual and concept features we used the CLIP [52] model (with the ViT B-32 as backbone) following the previous works [84, 82, 79]. For computing the pseudo-labels for label-free CS (in Sec. 4.3) we used a ViT L-14 CLIP model trained on the DataComp-1B dataset [27]. Further experimental details are mentioned in App. C.

CS baselines and methods: We compare our method against various baselines and SOTA CS methods. 1) **Random**: Uniformly select samples from the datasets to form the coreset. $\text{Random}_{\text{FFCV}}$ denotes the performance of the models trained on random subsets of Imagenet using FFCV [37]. 2) **Entropy [11]**: Selects samples based on entropy computed as the uncertainty of a model’s prediction on a sample. 3) **Forgetting [68]**: Selects samples based on the forgetting score computed as the number of times a sample is misclassified after being correctly classified earlier during training of the downstream model. A higher forgetting score indicates a more challenging sample. 4) **AUM [51]**: Selects samples based on their average margin during training of the downstream model i.e., the difference between the target class and the next highest class across the training epochs. Lower AUM indicates a more challenging sample. For forgetting, AUM, and our method, we use CCS [86] to form the coreset whereas for entropy we select samples with the highest entropy as done in [11, 86].

For label-free CS, we use 1) **Prototypicality [65]**: which first performs k-means clustering in the embedding space of SwAV [6] model and ranks samples based on their Euclidean distance to the

Table 1: Comparison of the model’s (RN-18 for CIFAR10/100 and RN-34 for Imagenet) test accuracy after training on coresets found by various approaches shows that our coresets lead to significantly better performance than Random achieving competitive results compared to the methods using the downstream model’s training dynamics, even for high pruning rates. (Best in each category is highlighted).

Method		Datasets and Pruning Rates											
		CIFAR-10				CIFAR-100				Imagenet			
		30%	50%	70%	90%	30%	50%	70%	90%	30%	50%	70%	90%
Needs downstream model training/dynamics	Entropy	94.44	92.11	85.67	66.52	72.26	63.26	50.49	28.96	72.34	70.76	64.04	39.04
	Forgetting	95.40	95.04	92.97	85.70	77.14	74.45	68.92	55.59	72.60	70.89	66.51	52.28
	AUM	95.27	94.93	93.00	86.08	76.84	73.77	68.85	55.03	72.29	70.52	67.78	57.36
Does not need downstream model training/dynamics	Random	94.33	93.40	90.94	79.08	74.59	71.07	65.30	44.76	72.18	70.34	66.67	52.34
	Random _{FFCV}	-	-	-	-	-	-	-	-	73.37 ± 0.08	71.71 ± 0.10	67.85 ± 0.04	51.29 ± 0.20
	Ours	94.77 ± 0.09	93.44 ± 0.61	91.80 ± 0.21	84.63 ± 0.24	75.98 ± 0.26	72.22 ± 0.22	66.53 ± 0.42	51.85 ± 0.29	73.39 ± 0.12	72.34 ± 0.13	69.44 ± 0.17	55.92 ± 0.02

Table 2: Comparison of the model’s test accuracy after training on coresets, found in a **label-free** manner, shows that our coresets lead to better performance than Random and Prototypicality. It is also competitive/better than the coresets found by ELFS (which uses training dynamics of the downstream model).

Method		Datasets and Pruning Rates											
		CIFAR-10				CIFAR-100				Imagenet			
		30%	50%	70%	90%	30%	50%	70%	90%	30%	50%	70%	90%
Needs downstream model training/dynamics	ELFS (SwAV)	95.00	94.30	91.80	82.50	76.10	72.10	65.50	49.80	73.20	71.40	66.80	53.40
	ELFS (DINO)	95.50	95.20	93.20	87.30	76.80	73.60	68.40	54.90	73.50	71.80	67.20	54.90
	Prototypicality	94.70	92.90	90.10	70.90	74.50	69.80	61.10	32.10	70.90	60.80	54.60	30.60
Does not need downstream model training/dynamics	Random	94.33	93.40	90.94	79.08	74.59	71.07	65.30	44.76	72.18	70.34	66.67	52.34
	Random _{FFCV}	-	-	-	-	-	-	-	-	73.37 ± 0.08	71.71 ± 0.10	67.85 ± 0.04	51.29 ± 0.20
	Ours-LF	94.81 ± 0.14	93.93 ± 0.13	91.75 ± 0.34	84.02 ± 0.44	74.67 ± 0.23	72.07 ± 0.38	65.50 ± 0.17	49.91 ± 0.96	73.61 ± 0.08	71.99 ± 0.05	68.42 ± 0.21	53.21 ± 0.06

cluster centers. Samples further away from the cluster center are used to form the coreset. 2) **ELFS** [87]: estimates the pseudo-labels of the unlabeled samples using a deep clustering approach (using the embedding space of SwAV [6] and DINO [7]) and forms the coreset using training dynamics of the downstream model trained on the pseudo-labeled data. Crucially, SOTA methods such as forgetting, AUM, and ELFS require training the downstream model on the entire dataset first for CS, unlike our method which is independent of the downstream model. While Random and Prototypicality also don’t require the downstream model for CS, our results show that our approach surpasses them.

5.1 Evaluating performance of our concept-based score for CS

Table 1 shows the accuracy of models trained on coresets found by various approaches on three datasets for the standard CS problem (where the dataset is labeled). Our results show that our coresets lead to significantly better performance, even at higher pruning rates, compared to the random subsets. Moreover, our method which does not have the knowledge of the downstream model or its training dynamics still provides competitive performance to coresets found by the SOTA approaches based on forgetting and AUM, and even outperforms them on Imagenet for smaller pruning rates.

Table 2 shows the accuracy of models trained on coresets when the training set is unlabeled (we report the numbers presented by [87] for previous methods). The results show that the random subsets are a competitive baseline for this problem outperforming Prototypicality [65]. Our results also show that our coresets outperform the random subsets for all pruning rates with significant improvements at higher pruning rates. Compared to ELFS [87], our method provides competitive performance and even surpasses it for lower pruning rates on Imagenet, without using any information about the downstream model’s architecture or its training dynamics highlighting its effectiveness.

Next, evaluate the transferability of the coresets found by our approach to downstream models with different architectures including those based on convolutional neural networks, ResNets and ViTs. Results in Table 3 and Table 13 (in App. C.4) show that our coresets achieve superior performance than random for all the architectures. Thus, our concept-based score in conjunction with stratified sampling [86] which balances the number of easy/hard examples in the coreset is an effective approach for both standard and label-free CS at various pruning rates.

5.2 Evaluating efficiency of CS via our concept-based approach

Here we compare the efficiency of our approach at finding coresets compared to approaches based on training dynamics. For training dynamics-based approaches the time required to find the coreset is

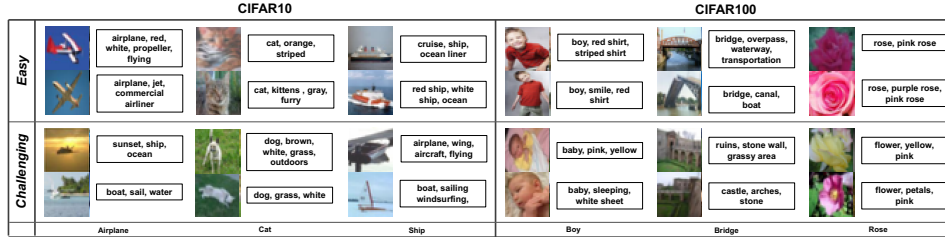


Figure 3: Visualizing samples according to our concept-based score for a subset of classes in CIFAR-10/100 showing that easy (challenging) samples are aligned (unaligned) with their assigned label. Image-level concepts (in boxes) extracted via LLaVA confirm that easy (challenging) examples are aligned (unaligned) with concepts of their labels, explaining the reason for a high (low) concept-based score.

dominated by the time needed to train the downstream model on the entire dataset first. For example, finding a coreset of Imagenet using a ResNet-34 model takes roughly 8 hours on two A-100 GPUs. In comparison, for our approach, extracting concepts via LLMs (block 1 of Fig. 2) takes 3 seconds per class (totaling to 25 minutes for all classes of Imagenet using 2 GPUs), and computing visual/concept features via CLIP and training a linear concept bottleneck layer (block 2 for Fig. 2) takes roughly 30 minutes for Imagenet offering $\approx 8\times$ speedup for CS over approaches relying on training dynamics of the downstream model. Moreover, since our method is independent of the downstream model architecture we do not need to repeat the CS step for different architectures. This is in contrast with training dynamics-based methods that require training the downstream model for every new architecture to find the corresponding best coreset for it.

5.3 Visualizing easy and challenging samples based on our concept-based score

Here we show the advantage of our concept-based score for assessing the sample’s difficulty and how using concepts aids its interpretability. We start by visualizing the easiest and the most challenging images (per class) for CIFAR-10/100. In Fig. 3, the top row shows the images with the highest concept-based scores (easiest) and the bottom shows the images with the lowest scores (challenging) for a subset of classes in CIFAR-10/100. As observed the easiest images are typical images associated with the label where as the challenging images are confusing (and even potentially mislabeled) as they look like images from a different class. For example, some challenging images in the class “boy” from CIFAR-100 are actually images of a baby which is also a class in CIFAR-100. Similarly, some challenging images from the class “cat” in CIFAR-10 look like images of a dog. More examples of such images are presented in Fig. 4 in App. C.1. Since the challenging examples seem to be confusing, it shows that our score can identify examples that are ambiguous or mislabeled. Such samples may be hard for some ML models to learn and could force them to rely on spurious features, potentially hurting generalization. The ability of our score to identify such samples without the downstream model demonstrates its effectiveness for ranking the samples for CS.

Table 3: Superior performance of downstream models with various architectures trained on our coresets for Imagenet compared to Random for standard (Ours) and label-free (Ours-LF) CS highlight our method’s effectiveness for CS without knowledge of the downstream model.

Model Architecture	Method	Pruning Rates			
		30%	50%	70%	90%
RN-18	Random	71.15 \pm 0.23	68.48 \pm 0.10	63.15 \pm 0.19	44.96 \pm 0.50
	Ours-LF	71.21 \pm 0.09	68.77 \pm 0.13	63.76 \pm 0.09	47.50 \pm 0.10
	Ours	70.94 \pm 0.19	69.30 \pm 0.84	65.16 \pm 0.04	49.57 \pm 0.16
RN-50	Random	76.06 \pm 0.11	74.44 \pm 0.04	70.50 \pm 0.02	53.56 \pm 0.13
	Ours-LF	76.54 \pm 0.08	74.84 \pm 0.03	71.10 \pm 0.09	55.22 \pm 0.92
	Ours	76.29 \pm 0.10	75.12 \pm 0.03	72.05 \pm 0.09	58.26 \pm 0.46
DenseNet	Random	76.55 \pm 0.11	75.31 \pm 0.15	71.85 \pm 0.20	56.27 \pm 0.21
	Ours-LF	76.94 \pm 0.23	75.52 \pm 0.11	72.28 \pm 0.14	58.16 \pm 0.04
	Ours	76.80 \pm 0.22	75.94 \pm 0.03	73.40 \pm 0.27	60.93 \pm 0.19
Wide Resnet	Random	77.39 \pm 0.19	75.32 \pm 0.12	71.51 \pm 0.10	54.78 \pm 0.83
	Ours-LF	77.83 \pm 0.08	75.77 \pm 0.09	71.97 \pm 0.08	57.34 \pm 0.58
	Ours	77.48 \pm 0.05	76.32 \pm 0.03	73.14 \pm 0.03	59.75 \pm 0.70

Next, we demonstrate why certain samples get low/high concept-based scores in our approach by extracting concepts specific to these images using LLaVA (note that these concepts are different from the per-class concepts used in the concept bottleneck). To generate these, we prompt LLaVA to produce concepts using both the sample image and its class label (see image-level concept extraction in App. B). These image-level concepts are shown in the boxes in Fig. 3. As observed in Fig. 3, image-level concepts provided by LLaVA are related to the class label for easy images whereas they

are unrelated for challenging images. For example, attributes provided by LLaVA for the challenging images of “airplane” align more with those of ship (both which are classes in CIFAR-10), and concepts provided for challenging images of “bridges” align more with those of castles (both of which are classes in CIFAR-100). Since our concept-based score in Eq. 4 assigns a small value for these images, we see that it correctly captures when a sample’s visual information is not aligned with the sample’s associated label and vice-versa. Thus, explaining why certain examples should be included/excluded from the coreset in an interpretable way independent of the downstream model.

5.4 Ablation studies

Here, we present ablation studies to evaluate various component of our approach. Specifically, we evaluate the effect of different 1) methods and LLMs used for concept generation, 2) number of concepts per class (k) in the bottleneck, 3) CLIP backbones for visual/concept similarity, 4) number of iterations (T) for training the concept bottleneck layer. Here we use CIFAR-100 with a 90% pruning ratio and train a ResNet-18 on the selected coresets. Lastly, we also evaluated the effectiveness of our method for CS on tasks beyond object recognition using medical and affective computing tasks.

Comparison of different techniques to generate concepts via LLaVA. Tables 4 and 5 shows how the performance of models trained on our coresets change when different method are used to generate the concept sets (Fig. 2 block 1). Since our method uses LLaVA [41], which is a VLM, we compare the performance of models trained on the random subsets and coresets obtained using class-wise concepts (only textual information) and concepts extracted using both visual and textual information.

For concepts generated using only textual information, we consider two alternatives, namely **class-wise attributes** (CW-A) and **class-wise descriptions** (CW-D). While CW-A considers concepts formed by a single or a few words, CW-D consists of longer, more descriptive concepts (eg., a descriptive concept for the class butterfly is “*a beautiful insect with colorful wings*”). For CW-D, we use a subset of k concepts provided by [82], generated via the GPT-3 model. Our results show that CW-A performs better than CW-D for both the standard/label-free CS problems. Thus, we used CW-A for all our experiments.

Next, for generating concepts using both visual and textual information, we consider two alternatives. The first is a **class-wise one-shot image attribute** approach where we first cluster all images of a class in the embedding space of the CLIP’s visual encoder and identify the image whose embedding is the closest to the cluster center (for the label-free setting we use the pseudo-labels of the images during clustering), then we prompt LLaVA to generate attributes using this single image and the class name. Once generated, we use k discriminative concepts to form the bottleneck. The second alternative is the **image-wise** attribute approach, where we use *each* image in the training set and prompt LLaVA to generate per image attributes describing the image. Once generated, we sort the concepts based on their frequency of occurrence in a class and use the most frequently occurring discriminative concepts to form the bottleneck. While the image-level concepts lead to the best coresets, it is slow and costly to prompt LLaVA to generate attributes for all the images in a large dataset such as Imagenet.

For CIFAR-100, this process took about nine hours to complete (in comparison CW-A can be extracted in 5 minutes without parallel computation) which is very costly compared to the small performance gains it provides over other approaches. Lastly, while the class-wise one-shot image attribute approach is better than CW-A, the additional step of clustering can be costly for larger datasets such as Imagenet. Based on these results, we used CW-A for concept generation using LLaVA.

Effect of k and the method for selecting k concepts. In Table 6, we show how the number of concepts extracted per class label, for creating the bottleneck in block 1 of Fig. 2 affects the selection

Table 4: Effect of using concepts obtained using only textual information (attributes vs. descriptions) to form the concept bottleneck layer ².

	class-wise attributes	class-wise descriptions
Ours	51.85 \pm 0.51	51.05 \pm 0.71
Ours-LF	49.91 \pm 0.96	49.85 \pm 0.83

Table 5: Effect of using concepts generated by using both visual and textual information to form the concept bottleneck layer ².

	class-wise one-shot image attributes	image-wise attributes
Ours	51.68 \pm 0.45	52.47 \pm 0.39
Ours-LF	50.22 \pm 0.16	51.05 \pm 0.93

Table 6: Effect of the number of per-class concepts k and the method of selecting k attribute-level concepts from those generated by LLaVA on the accuracy of models trained on the coreset².

Concept selection	$k=1$	$k=5$	$k=10$
Random concepts	48.78 \pm 0.96	50.15 \pm 1.64	50.39 \pm 0.72
Discriminative	51.42 \pm 0.18	51.85 \pm 0.29	51.22 \pm 0.72

²Cf. A random subset of CIFAR-100 achieves an accuracy of 44.76 \pm 1.58 at 90% pruning rate.

Table 7: Effect of using different LLMs for generating concepts used in the concept bottleneck².

LLM	Accuracy
GPT-3	51.05 \pm 0.71
Phi-3	51.30 \pm 0.26
LLaVA	51.85 \pm 0.29

Table 8: Effect² of using various CLIP backbones for computing the visual-concept similarity in Eq. 2.

CLIP backbone	Accuracy
ViT B-16	48.89 \pm 1.01
ViT L-14	49.54 \pm 1.82
ResNet-50	50.56 \pm 1.67
ViT B-32	51.85 \pm 0.29

Table 9: Effect² of using different number training epochs T for computing the score in Eq. 4.

T	Accuracy
10	46.63 \pm 0.08
20	48.40 \pm 0.10
50	50.50 \pm 0.31
100	51.85 \pm 0.29

of coresets. Once the list of class-wise attribute-level concepts is generated by LLaVA, we can select k concepts per class either randomly or choose concepts unique to a class (discriminative). Our results show that using even $k = 1$ is sufficient to surpass the performance using a random subset². This performance increases when we keep discriminative concepts in our concept bottleneck, with $k = 5$ achieving the best results. While the size of the concept bottleneck need not be large to find good coresets, it is helpful to take a sample’s visual similarity with a set of concepts rather than a single concept per class. Thus, we used 5 discriminative concepts per class to form the bottleneck.

Effect of using different LLMs/VLMs for concept extraction. We evaluated three different VLMs for concept extraction in block 1 of Fig. 2. We used GPT-3 and two open source VLMs namely Phi-3-Mini-4K-Instruct with 3.8 billion parameters, and LLaVA with 7 billion parameters. In Table 7, we find that the performance of our method remains stable regardless of the LLM used, indicating that even smaller LLMs are effective at generating concepts that produce high performing coresets.

Effect of using different VLMs for measuring visual and concept similarity. Here we evaluated different CLIP backbones to compute the similarity between the visual and concept features used in Eq. 2 (block 2 of Fig. 2). Our results in Table 8 show that our concept-based method achieves significantly better performance than Random² for all the backbones with ViT B-32 backbone performing the best. Thus, we used this backbone for all the experiments in the paper.

Effect of number of epochs T . Here we evaluated the effect of using different number of epochs T used for training the concept bottleneck layer for computing the concept-based score. Our results in Table 9 show that $T \geq 50$ is enough to achieve concept-based scores that lead to selection of high performing coresets. We used $T = 100$ in our experiments since that achieves the best performance.

Evaluation on medical and affective computing tasks. In App. C.2, we present an evaluation of using our approach for CS for biomedical entity recognition (using BloodMNIST [1]) and emotion recognition (using a subset of AffectNet [45]) task. Superior performance of our approach in Tables 10 and 11 on these tasks highlights the effectiveness of our approach for CS on diverse tasks.

6 Conclusion

CS finds representative samples from a large dataset, training models on which leads to models with accuracy similar to the models trained on the entire dataset. In this work, we proposed a scoring mechanism based on concept bottlenecks that allows us to compute the difficulty of a sample in terms of interpretable concepts. This method is independent of the downstream model and avoids training the downstream model on the full dataset even once. Our experiments show that training downstream models on coresets selected using our approach leads to better performance than random subsets and achieves accuracy similar to or better than the SOTA approaches based on training dynamics of the downstream model, for both the standard and label-free CS problem. Moreover, our score provides an intuitive explanation of a sample’s difficulty at a dataset level, independent of the downstream model.

Limitations: While we evaluated various LLMs for concept generation and showed their effectiveness for computing concept-based score, it is possible that for some classes LLMs produce very noisy and non-discriminative concepts, leading to poor concept-based scores. Thus, developing methods to prompt the LLMs to generate discriminative concepts to be used as the concept bottleneck is a crucial research direction and is left for future works. Another limitation is the dependence of our score on the VLMs for computing similarity between visual and concept features. Although we evaluated our approach on a diverse set of tasks including a biomedical task and various CLIP-based VLMs, it is possible that these similarity scores may not work well for certain tasks, warranting additional fine-tuning to make the similarity scores meaningful. Hence, in practice, additional time/compute may be required to identify or fine-tune a VLM for CS.

References

- [1] Andrea Acevedo, Anna Merino, Santiago Alf  rez,   ngel Molina, Laura Bold  , and Jos   Rodellar. A dataset of microscopic peripheral blood cell images for development of automatic recognition systems. *Data in brief*, 30:105474, 2020.
- [2] Josh Achiam, Steven Adler, Sandhini Agarwal, Lama Ahmad, Ilge Akkaya, Florencia Leoni Aleman, Diogo Almeida, Janko Altschmidt, Sam Altman, Shyamal Anadkat, et al. Gpt-4 technical report. *arXiv preprint arXiv:2303.08774*, 2023.
- [3] David Bau, Bolei Zhou, Aditya Khosla, Aude Oliva, and Antonio Torralba. Network dissection: Quantifying interpretability of deep visual representations. In *Proceedings of the IEEE conference on computer vision and pattern recognition*, pages 6541–6549, 2017.
- [4] Usha Bhalla, Alex Oesterling, Suraj Srinivas, Flavio P Calmon, and Himabindu Lakkaraju. Interpreting clip with sparse linear concept embeddings (splice). *arXiv preprint arXiv:2402.10376*, 2024.
- [5] Sebastian Bujwid and Josephine Sullivan. Large-scale zero-shot image classification from rich and diverse textual descriptions. *arXiv preprint arXiv:2103.09669*, 2021.
- [6] Mathilde Caron, Ishan Misra, Julien Mairal, Priya Goyal, Piotr Bojanowski, and Armand Joulin. Unsupervised learning of visual features by contrasting cluster assignments. *Advances in neural information processing systems*, 33:9912–9924, 2020.
- [7] Mathilde Caron, Hugo Touvron, Ishan Misra, Herv   J  gou, Julien Mairal, Piotr Bojanowski, and Armand Joulin. Emerging properties in self-supervised vision transformers. In *Proceedings of the IEEE/CVF international conference on computer vision*, pages 9650–9660, 2021.
- [8] Samprit Chatterjee and Ali S Hadi. Influential observations, high leverage points, and outliers in linear regression. *Statistical science*, pages 379–393, 1986.
- [9] Chaofan Chen, Oscar Li, Daniel Tao, Alina Barnett, Cynthia Rudin, and Jonathan K Su. This looks like that: deep learning for interpretable image recognition. *Advances in neural information processing systems*, 32, 2019.
- [10] Hoyong Choi, Nohyun Ki, and Hye Won Chung. Bws: Best window selection based on sample scores for data pruning across broad ranges. *arXiv preprint arXiv:2406.03057*, 2024.
- [11] Cody Coleman, Christopher Yeh, Stephen Mussmann, Baharan Mirzasoleiman, Peter Bailis, Percy Liang, Jure Leskovec, and Matei Zaharia. Selection via proxy: Efficient data selection for deep learning. *arXiv preprint arXiv:1906.11829*, 2019.
- [12] Aron Culotta and Andrew McCallum. Reducing labeling effort for structured prediction tasks. In *AAAI*, volume 5, pages 746–751, 2005.
- [13] Jia Deng, Wei Dong, Richard Socher, Li-Jia Li, Kai Li, and Li Fei-Fei. Imagenet: A large-scale hierarchical image database. In *2009 IEEE conference on computer vision and pattern recognition*, pages 248–255. Ieee, 2009.
- [14] Alexey Dosovitskiy, Lucas Beyer, Alexander Kolesnikov, Dirk Weissenborn, Xiaohua Zhai, Thomas Unterthiner, Mostafa Dehghani, Matthias Minderer, Georg Heigold, Sylvain Gelly, et al. An image is worth 16x16 words: Transformers for image recognition at scale. *arXiv preprint arXiv:2010.11929*, 2020.
- [15] Dan Feldman and Michael Langberg. A unified framework for approximating and clustering data. In *Proceedings of the forty-third annual ACM symposium on Theory of computing*, pages 569–578, 2011.
- [16] Dan Feldman, Melanie Schmidt, and Christian Sohler. Turning big data into tiny data: Constant-size coresets for k-means, pca, and projective clustering. *SIAM Journal on Computing*, 49(3):601–657, 2020.
- [17] Brent A Griffin, Jacob Marks, and Jason J Corso. Zero-shot coreset selection: Efficient pruning for unlabeled data. *arXiv preprint arXiv:2411.15349*, 2024.

- [18] Chengcheng Guo, Bo Zhao, and Yanbing Bai. Deepcore: A comprehensive library for coreset selection in deep learning. In *International Conference on Database and Expert Systems Applications*, pages 181–195. Springer, 2022.
- [19] Kaiming He, Xiangyu Zhang, Shaoqing Ren, and Jian Sun. Deep residual learning for image recognition. In *Proceedings of the IEEE conference on computer vision and pattern recognition*, pages 770–778, 2016.
- [20] Lisa Anne Hendricks, Zeynep Akata, Marcus Rohrbach, Jeff Donahue, Bernt Schiele, and Trevor Darrell. Generating visual explanations. In *Computer Vision–ECCV 2016: 14th European Conference, Amsterdam, The Netherlands, October 11–14, 2016, Proceedings, Part IV 14*, pages 3–19. Springer, 2016.
- [21] Lisa Anne Hendricks, Ronghang Hu, Trevor Darrell, and Zeynep Akata. Grounding visual explanations. In *Proceedings of the European conference on computer vision (ECCV)*, pages 264–279, 2018.
- [22] Tom Henighan, Jared Kaplan, Mor Katz, Mark Chen, Christopher Hesse, Jacob Jackson, Heewoo Jun, Tom B Brown, Prafulla Dhariwal, Scott Gray, et al. Scaling laws for autoregressive generative modeling. *arXiv preprint arXiv:2010.14701*, 2020.
- [23] Evan Hernandez, Sarah Schwettmann, David Bau, Teona Bagashvili, Antonio Torralba, and Jacob Andreas. Natural language descriptions of deep visual features. In *International Conference on Learning Representations*, 2021.
- [24] Joel Hestness, Sharan Narang, Newsha Ardalani, Gregory Diamos, Heewoo Jun, Hassan Kianinejad, Md Mostofa Ali Patwary, Yang Yang, and Yanqi Zhou. Deep learning scaling is predictable, empirically. *arXiv preprint arXiv:1712.00409*, 2017.
- [25] Gao Huang, Zhuang Liu, Laurens Van Der Maaten, and Kilian Q Weinberger. Densely connected convolutional networks. In *Proceedings of the IEEE conference on computer vision and pattern recognition*, pages 4700–4708, 2017.
- [26] Lingxiao Huang, Shaofeng Jiang, and Nisheeth Vishnoi. Coresets for clustering with fairness constraints. *Advances in neural information processing systems*, 32, 2019.
- [27] Gabriel Ilharco, Mitchell Wortsman, Ross Wightman, Cade Gordon, Nicholas Carlini, Rohan Taori, Achal Dave, Vaishaal Shankar, Hongseok Namkoong, John Miller, Hannaneh Hajishirzi, Ali Farhadi, and Ludwig Schmidt. Openclip. <https://doi.org/10.5281/zenodo.5143773>, July 2021. If you use this software, please cite it as below.
- [28] Jared Kaplan, Sam McCandlish, Tom Henighan, Tom B Brown, Benjamin Chess, Rewon Child, Scott Gray, Alec Radford, Jeffrey Wu, and Dario Amodei. Scaling laws for neural language models. *arXiv preprint arXiv:2001.08361*, 2020.
- [29] Jihyung Kil and Wei-Lun Chao. Revisiting document representations for large-scale zero-shot learning. *arXiv preprint arXiv:2104.10355*, 2021.
- [30] Krishnateja Killamsetty, Sivasubramanian Durga, Ganesh Ramakrishnan, Abir De, and Rishabh Iyer. Grad-match: Gradient matching based data subset selection for efficient deep model training. In *International Conference on Machine Learning*, pages 5464–5474. PMLR, 2021.
- [31] Krishnateja Killamsetty, Alexandre V Evfimievski, Tejaswini Pedapati, Kiran Kate, Lucian Popa, and Rishabh Iyer. Milo: Model-agnostic subset selection framework for efficient model training and tuning. *arXiv preprint arXiv:2301.13287*, 2023.
- [32] Jinkyu Kim, Anna Rohrbach, Trevor Darrell, John Canny, and Zeynep Akata. Textual explanations for self-driving vehicles. In *Proceedings of the European conference on computer vision (ECCV)*, pages 563–578, 2018.
- [33] Pang Wei Koh and Percy Liang. Understanding black-box predictions via influence functions. In *International conference on machine learning*, pages 1885–1894. PMLR, 2017.

- [34] Pang Wei Koh, Thao Nguyen, Yew Siang Tang, Stephen Mussmann, Emma Pierson, Been Kim, and Percy Liang. Concept bottleneck models. In *International conference on machine learning*, pages 5338–5348. PMLR, 2020.
- [35] Alex Krizhevsky, Geoffrey Hinton, et al. Learning multiple layers of features from tiny images. *arXiv preprint arXiv:1206.5808*, 2009.
- [36] Christoph H Lampert, Hannes Nickisch, and Stefan Harmeling. Attribute-based classification for zero-shot visual object categorization. *IEEE transactions on pattern analysis and machine intelligence*, 36(3):453–465, 2013.
- [37] Guillaume Leclerc, Andrew Ilyas, Logan Engstrom, Sung Min Park, Hadi Salman, and Aleksander Madry. Ffcv: Accelerating training by removing data bottlenecks. In *Proceedings of the IEEE/CVF Conference on Computer Vision and Pattern Recognition*, pages 12011–12020, 2023.
- [38] David D Lewis and Jason Catlett. Heterogeneous uncertainty sampling for supervised learning. In *Machine learning proceedings 1994*, pages 148–156. Elsevier, 1994.
- [39] Jeffrey Li, Alex Fang, Georgios Smyrnis, Maor Ivgi, Matt Jordan, Samir Yitzhak Gadre, Hritik Bansal, Etash Guha, Sedrick Scott Keh, Kushal Arora, et al. Datacomp-lm: In search of the next generation of training sets for language models. *Advances in Neural Information Processing Systems*, 37:14200–14282, 2024.
- [40] Haotian Liu, Chunyuan Li, Yuheng Li, and Yong Jae Lee. Improved baselines with visual instruction tuning, 2023.
- [41] Haotian Liu, Chunyuan Li, Qingyang Wu, and Yong Jae Lee. Visual instruction tuning. In *NeurIPS*, 2023.
- [42] Zhuoming Liu, Hao Ding, Huaping Zhong, Weijia Li, Jifeng Dai, and Conghui He. Influence selection for active learning. In *Proceedings of the IEEE/CVF international conference on computer vision*, pages 9274–9283, 2021.
- [43] Adyasha Maharana, Prateek Yadav, and Mohit Bansal. D2 pruning: Message passing for balancing diversity and difficulty in data pruning. *arXiv preprint arXiv:2310.07931*, 2023.
- [44] Baharan Mirzasoleiman, Jeff Bilmes, and Jure Leskovec. Coresets for data-efficient training of machine learning models. In *International Conference on Machine Learning*, pages 6950–6960. PMLR, 2020.
- [45] Ali Mollahosseini, Behzad Hasani, and Mohammad H Mahoor. Affectnet: A database for facial expression, valence, and arousal computing in the wild. *IEEE Transactions on Affective Computing*, 10(1):18–31, 2017.
- [46] Jesse Mu and Jacob Andreas. Compositional explanations of neurons. *Advances in Neural Information Processing Systems*, 33:17153–17163, 2020.
- [47] Meike Nauta, Ron Van Bree, and Christin Seifert. Neural prototype trees for interpretable fine-grained image recognition. In *Proceedings of the IEEE/CVF conference on computer vision and pattern recognition*, pages 14933–14943, 2021.
- [48] Kosuke Nishida, Kyosuke Nishida, and Shuichi Nishioka. Improving few-shot image classification using machine-and user-generated natural language descriptions. *arXiv preprint arXiv:2207.03133*, 2022.
- [49] Dong Huk Park, Lisa Anne Hendricks, Zeynep Akata, Anna Rohrbach, Bernt Schiele, Trevor Darrell, and Marcus Rohrbach. Multimodal explanations: Justifying decisions and pointing to the evidence. In *Proceedings of the IEEE conference on computer vision and pattern recognition*, pages 8779–8788, 2018.
- [50] Mansheej Paul, Surya Ganguli, and Gintare Karolina Dziugaite. Deep learning on a data diet: Finding important examples early in training. *Advances in neural information processing systems*, 34:20596–20607, 2021.

- [51] Geoff Pleiss, Tianyi Zhang, Ethan Elenberg, and Kilian Q Weinberger. Identifying mislabeled data using the area under the margin ranking. *Advances in Neural Information Processing Systems*, 33:17044–17056, 2020.
- [52] Alec Radford, Jong Wook Kim, Chris Hallacy, Aditya Ramesh, Gabriel Goh, Sandhini Agarwal, Girish Sastry, Amanda Askell, Pamela Mishkin, Jack Clark, et al. Learning transferable visual models from natural language supervision. In *International conference on machine learning*, pages 8748–8763. PMLR, 2021.
- [53] Jonathan S Rosenfeld, Amir Rosenfeld, Yonatan Belinkov, and Nir Shavit. A constructive prediction of the generalization error across scales. *arXiv preprint arXiv:1909.12673*, 2019.
- [54] Karsten Roth, Oriol Vinyals, and Zeynep Akata. Integrating language guidance into vision-based deep metric learning. In *Proceedings of the IEEE/CVF Conference on Computer Vision and Pattern Recognition*, pages 16177–16189, 2022.
- [55] Olga Russakovsky and Li Fei-Fei. Attribute learning in large-scale datasets. In *Trends and Topics in Computer Vision: ECCV 2010 Workshops, Heraklion, Crete, Greece, September 10-11, 2010, Revised Selected Papers, Part I 11*, pages 1–14. Springer, 2012.
- [56] Mark Sandler, Andrew Howard, Menglong Zhu, Andrey Zhmoginov, and Liang-Chieh Chen. Mobilenetv2: Inverted residuals and linear bottlenecks. In *Proceedings of the IEEE conference on computer vision and pattern recognition*, pages 4510–4520, 2018.
- [57] Victor Garcia Satorras and Joan Bruna Estrach. Few-shot learning with graph neural networks. In *International conference on learning representations*, 2018.
- [58] Andrea Schioppa, Polina Zablotskaia, David Vilar, and Artem Sokolov. Scaling up influence functions. In *Proceedings of the AAAI Conference on Artificial Intelligence*, volume 36, pages 8179–8186, 2022.
- [59] Ramprasaath R Selvaraju, Michael Cogswell, Abhishek Das, Ramakrishna Vedantam, Devi Parikh, and Dhruv Batra. Grad-cam: Visual explanations from deep networks via gradient-based localization. In *Proceedings of the IEEE international conference on computer vision*, pages 618–626, 2017.
- [60] Ozan Sener and Silvio Savarese. Active learning for convolutional neural networks: A core-set approach. *arXiv preprint arXiv:1708.00489*, 2017.
- [61] Burr Settles. Active learning. *Synthesis Lectures on Artificial Intelligence and Machine Learning*, 6(1):1–114, June 2012.
- [62] Sheng Shen, Chunyuan Li, Xiaowei Hu, Yujia Xie, Jianwei Yang, Pengchuan Zhang, Zhe Gan, Lijuan Wang, Lu Yuan, Ce Liu, et al. K-lite: Learning transferable visual models with external knowledge. *Advances in Neural Information Processing Systems*, 35:15558–15573, 2022.
- [63] Chandan Singh, John X Morris, Jyoti Aneja, Alexander M Rush, and Jianfeng Gao. Explaining data patterns in natural language with language models. In *Proceedings of the 6th BlackboxNLP Workshop: Analyzing and Interpreting Neural Networks for NLP*, pages 31–55, 2023.
- [64] Jake Snell, Kevin Swersky, and Richard Zemel. Prototypical networks for few-shot learning. *Advances in neural information processing systems*, 30, 2017.
- [65] Ben Sorscher, Robert Geirhos, Shashank Shekhar, Surya Ganguli, and Ari Morcos. Beyond neural scaling laws: beating power law scaling via data pruning. *Advances in Neural Information Processing Systems*, 35:19523–19536, 2022.
- [66] Robyn Speer, Joshua Chin, and Catherine Havasi. Conceptnet 5.5: An open multilingual graph of general knowledge. In *Proceedings of the AAAI conference on artificial intelligence*, volume 31, 2017.
- [67] Mingxing Tan and Quoc Le. Efficientnet: Rethinking model scaling for convolutional neural networks. In *International conference on machine learning*, pages 6105–6114. PMLR, 2019.

- [68] Mariya Toneva, Alessandro Sordoni, Remi Tachet des Combes, Adam Trischler, Yoshua Bengio, and Geoffrey J Gordon. An empirical study of example forgetting during deep neural network learning. *arXiv preprint arXiv:1812.05159*, 2018.
- [69] Hugo Touvron, Matthieu Cord, Matthijs Douze, Francisco Massa, Alexandre Sablayrolles, and Hervé Jégou. Training data-efficient image transformers & distillation through attention. In *International conference on machine learning*, pages 10347–10357. PMLR, 2021.
- [70] Hugo Touvron, Thibaut Lavril, Gautier Izacard, Xavier Martinet, Marie-Anne Lachaux, Timothée Lacroix, Baptiste Rozière, Naman Goyal, Eric Hambro, Faisal Azhar, et al. Llama: Open and efficient foundation language models. *arXiv preprint arXiv:2302.13971*, 2023.
- [71] Murad Tukan, Samson Zhou, Alaa Maalouf, Daniela Rus, Vladimir Braverman, and Dan Feldman. Provable data subset selection for efficient neural networks training. In *International Conference on Machine Learning*, pages 34533–34555. PMLR, 2023.
- [72] Oriol Vinyals, Charles Blundell, Timothy Lillicrap, Daan Wierstra, et al. Matching networks for one shot learning. *Advances in neural information processing systems*, 29, 2016.
- [73] Yan Wang, Wei Song, Wei Tao, Antonio Liotta, Dawei Yang, Xinlei Li, Shuyong Gao, Yixuan Sun, Weifeng Ge, Wei Zhang, et al. A systematic review on affective computing: Emotion models, databases, and recent advances. *Information Fusion*, 83:19–52, 2022.
- [74] Sandareka Wickramanayake, Wynne Hsu, and Mong Li Lee. Explanation-based data augmentation for image classification. *Advances in neural information processing systems*, 34:20929–20940, 2021.
- [75] Mitchell Wortsman, Gabriel Ilharco, Jong Wook Kim, Mike Li, Simon Kornblith, Rebecca Roelofs, Raphael Gontijo Lopes, Hannaneh Hajishirzi, Ali Farhadi, Hongseok Namkoong, et al. Robust fine-tuning of zero-shot models. In *Proceedings of the IEEE/CVF conference on computer vision and pattern recognition*, pages 7959–7971, 2022.
- [76] Qi Wu, Chunhua Shen, Lingqiao Liu, Anthony Dick, and Anton van den Hengel. What value do explicit high level concepts have in vision to language problems?, 2016.
- [77] Xiaobo Xia, Jiale Liu, Jun Yu, Xu Shen, Bo Han, and Tongliang Liu. Moderate coreset: A universal method of data selection for real-world data-efficient deep learning. In *The Eleventh International Conference on Learning Representations*, 2022.
- [78] Wenjia Xu, Yongqin Xian, Jiuniu Wang, Bernt Schiele, and Zeynep Akata. Attribute prototype network for zero-shot learning. *Advances in Neural Information Processing Systems*, 33:21969–21980, 2020.
- [79] An Yan, Yu Wang, Yiwu Zhong, Chengyu Dong, Zexue He, Yujie Lu, William Yang Wang, Jingbo Shang, and Julian McAuley. Learning concise and descriptive attributes for visual recognition. In *Proceedings of the IEEE/CVF International Conference on Computer Vision*, pages 3090–3100, 2023.
- [80] Jiancheng Yang, Rui Shi, and Bingbing Ni. Medmnist classification decathlon: A lightweight automl benchmark for medical image analysis. In *IEEE 18th International Symposium on Biomedical Imaging (ISBI)*, pages 191–195, 2021.
- [81] Jiancheng Yang, Rui Shi, Donglai Wei, Zequan Liu, Lin Zhao, Bilian Ke, Hanspeter Pfister, and Bingbing Ni. Medmnist v2-a large-scale lightweight benchmark for 2d and 3d biomedical image classification. *Scientific Data*, 10(1):41, 2023.
- [82] Yue Yang, Artemis Panagopoulou, Shenghao Zhou, Daniel Jin, Chris Callison-Burch, and Mark Yatskar. Language in a bottle: Language model guided concept bottlenecks for interpretable image classification. In *Proceedings of the IEEE/CVF Conference on Computer Vision and Pattern Recognition*, pages 19187–19197, 2023.
- [83] Mert Yuksekgonul, Maggie Wang, and James Zou. Post-hoc concept bottleneck models. *arXiv preprint arXiv:2205.15480*, 2022.

- [84] Tian Yun, Usha Bhalla, Ellie Pavlick, and Chen Sun. Do vision-language pretrained models learn composable primitive concepts? *arXiv preprint arXiv:2203.17271*, 2022.
- [85] Sergey Zagoruyko and Nikos Komodakis. Wide residual networks. *arXiv preprint arXiv:1605.07146*, 2016.
- [86] Haizhong Zheng, Rui Liu, Fan Lai, and Atul Prakash. Coverage-centric coreset selection for high pruning rates. *arXiv preprint arXiv:2210.15809*, 2022.
- [87] Haizhong Zheng, Elisa Tsai, Yifu Lu, Jiachen Sun, Brian R Bartoldson, Bhavya Kailkhura, and Atul Prakash. Elfs: Enhancing label-free coreset selection via clustering-based pseudo-labeling. *arXiv preprint arXiv:2406.04273*, 2024.

Appendix

We present additional related work in Appendix A. Then we describe the details of our methodology for extracting the concepts from LLaVA in Appendix B and present additional experiments and implementation details of our experiments in Appendix C including the algorithm for stratified sampling used in our work in Appendix C.5.

A Additional related work

Concept-based interpretability: Interpretability methods can be broadly classified as *post-hoc methods* (do not impose any model constraints) or *by-design* methods. Post-hoc methods include Gradient-weighted Class Activation Mapping approaches [3, 59, 46, 23] that trace network gradients to identify the input areas that guide predictions and Explanation Generation methods [63, 48, 32, 20] that require models to produce explanations for visual tasks by conditioning their predictions on captioning models or incorporating visual evidence to ground explanations [21, 49]. Interpretable-by-design methods, such as Prototype methods, optimize a metric space where classifications are based on distances to class prototypes, identifying important input regions but often obscuring their semantic content [47, 9, 64, 57, 72].

Concept Bottleneck Models (CBMs) are a part of interpretable-by-design approaches that use human-understandable attributes as an intermediate layer for predictions. A recent advancement, Computational Derivation Learning (CompDL), utilizes a CBM architecture by applying a linear layer over CLIP scores between expert-designed concepts and images, improving evaluation of how well CLIP grounds concepts [84]. Post-hoc Concept Bottleneck Models (PCBMs) were recently proposed to ease the requirement of CBMs to rely on costly concept annotations and improve their accuracy compared to end-to-end models. However, PCBMs are limited by the coverage of knowledge bases, making them unsuitable for large-scale or domain-specific tasks or fine-grained classification, and their residual predictors can undermine interpretability by blending CBMs with end-to-end models.

High-level semantic-driven descriptions are also used to guide data augmentation to build an informative set [74] to make model training efficient with a good enough training set. Prior works use external knowledge bases to obtain these textual semantic concepts to guide vision models [5, 29, 54, 62]. Thus, the use of concepts has been shown to improve interpretability in various domains. However, to the best of our knowledge, we are the first ones to propose a concept-based score for the CS problem and show its competitiveness to SOTA model training dynamics-dependent approaches.

Adaptive subset selection: These works focus of improving the training convergence and efficiency of model training by selecting a new subset of data from the whole dataset, every epoch, while training a downstream model. Thus, unlike our work, these works do not prune the dataset but rather keep selecting small, potentially non-overlapping, subsets every few epochs. Both [31, 71], propose ways to select subsets every epoch or every few epochs in a way that does not use a downstream model unlike some other works such as GradMatch [30], which select subsets based on the downstream model. While our work does not target adaptive subset selection, we evaluated how well our approach performs without any change on this problem in App. C.3. Our results show that, even on for this application, our concept-based score is an effective method.

B Details for concept set generation

Prompt Selection: To extract concepts for our approach, we only use the class labels in the prompt as can be seen in Figure 2. The prompt, “Can you give distinct attributes for <class name>. Give the output separated by a comma in the line.” instructs the VLM not only to provide distinct keywords but also adds formatting instructions. However, despite the instructions included in the prompt, LLaVA outputs are not always formatted well, often containing duplicate entries, mismatched commas and braces, and sometimes having a detailed explanation before the keywords. To remedy this we run the LLaVA output through a simple post-processing script and use regular expressions to clean the LLaVA outputs. For our experiments where we perform ablation of various concept-bottleneck generation methods (Tables 4, 5), we also use two more concept generation methods, one is one-shot image-based class concepts and the second is image-level concept generation. For the former, where we select one representative image per class via clustering, we prompt LLaVA as follows, “(image)

Table 10: Performance of concept-based coreset selection for emotion recognition task on Affectnet dataset. Coresets selected by our approach results in superior performance (higher F1 score) compared to Random for standard CS.

Model Arch.	Method	Pruning Rates			
		30%	50%	70%	90%
EfficientNet	Random	0.607 \pm 0.006	0.573 \pm 0.025	0.517 \pm 0.006	0.347 \pm 0.055
	Ours	0.603 \pm 0.006	0.577 \pm 0.021	0.537 \pm 0.015	0.450 \pm 0.035

Table 11: Performance of concept-based coreset selection for biomedical image recognition task on BloodM-NIST dataset. Coresets selected by our approach results in superior accuracy compared to Random for standard CS, highlighting our method’s effectiveness across various tasks.

Model Arch.	Method	Pruning Rates			
		30%	50%	70%	90%
ResNet-18	Random	94.99 \pm 0.27	94.79 \pm 0.18	91.71 \pm 0.29	86.50 \pm 0.66
	Ours	94.64 \pm 0.60	94.06 \pm 0.10	92.26 \pm 0.19	87.44 \pm 1.46

Can you give distinct attributes for such an image of \langle class name \rangle . Give the output separated by a comma in the line.” And, to get concepts for every image of a class, we use a similar prompt as follows, “ \langle image \rangle Can you give distinct visual attributes for this image of \langle class name \rangle . Give the output separated by a comma in the line.” Each LLaVA prompt request on a single A-100 GPU takes approximately 3 seconds.

Alternative VLMs for Concept Generation: We leverage LLaVA as our choice of VLM for concept generation, however in Table 7, we also compared against concepts extracted from GPT [79] and another smaller open source VLM (Phi-3-Mini-4K-Instruct). We see comparable performance of our CS method with concepts extracted from these models. We also experimented with retrieving concepts via another recent method, SpLiCE [4] which uses a linear optimization for sparse concept decomposition. However, a major limitation of SpLiCE is that similar to image-wise attributes as used in Table 5 it is a costly approach (SpLiCE can take up to 3 hours for 50,000 images, significantly slower than generating class-level concepts from LLaVA).

C Additional experiments and implementation details

C.1 Visualizing easy/challenging samples based on concept-based score

Similar to Fig 3 in Sec. 5.3 of the main paper, we visualize easy and challenging examples in Fig. 4 for CIFAR-10 and subset of classes from CIFAR-100. As observed the easy images (the ones that get high scores in our approach) are more canonical images of the class labels whereas the challenging ones are images that can potentially be assigned another class in the same dataset or are mislabeled in the dataset. The clear distinctions between these images show that our concept-based score aligns well with human intuition on the difficulty of the samples.

C.2 Concept-based CS for emotion recognition and biomedical image recognition

To validate the effectiveness of our concept-based coreset selection method beyond object recognition tasks, we apply our concept-based CS approach to the task of emotion recognition and biomedical image recognition.

For emotion recognition, we use the Affectnet dataset [45] for our experiments. AffectNet is a large-scale facial expression dataset designed for training and evaluating affective computing models [73]. It contains facial images collected from the internet using web search queries for emotion-related keywords in multiple languages. Each image is manually annotated for eight discrete emotion categories: neutral, happiness, sadness, surprise, fear, disgust, anger, contempt. For our experiments, we utilize an openly available version of this dataset³, containing roughly 16000 training and 14000 testing samples.

³<https://www.kaggle.com/datasets/noamsegal/affectnet-training-data>

Table 12: Adaptive coreset selection (Results for RBFNN and GradMatchPB are taken from tables 1 and 3 of Tukan et. al.)

Method	Datasets and Pruning Rates			
	CIFAR-10		CIFAR-100	
	70%	90%	70%	90%
GradMatchPB [30]	91.89	90.01	72.57	60.39
RBFNN [71]	94.44	91.40	73.48	64.59
Adaptive Random	93.64 ± 0.21	90.49 ± 0.41	71.70 ± 0.30	61.24 ± 0.37
Ours (adaptive)	92.61 ± 0.08	89.95 ± 0.26	71.74 ± 0.33	63.71 ± 0.48

According to our approach we first use LLaVA to extract concepts for the 8 emotion classes, using the following prompt, “*What are the facial features that distinguish emotion class name from other emotion types. Focus on changes in eyes, nose, lips, eyebrows, mouth. Give the output separated by commas in a line.*”. We get 5 – 10 distinctive facial feature concepts for every emotion, for instance for emotion class *happy*, we get the following concepts, “*wide open eyes*”, “*sparkling eyes*”, “*smiling lips*”, “*open mouth*”, “*raised eyebrows*”, “*flushed cheeks*”, “*teeth barred*”. We finally select $k = 5$ discriminative concepts from this list.

To test coreset performance, we use the EfficientNet model [67] and report F1 scores for our coresets in Table 10. When compared against randomly selected coresets for the various pruning ratios, coresets selected via our concept-based approach achieve better performance.

For biomedical image recognition, we use the BloodMNIST [1] dataset from the MedMNIST [80, 81] which comprises of images of normal blood cells, captured from individuals without infection, hematologic or oncologic disease and free of any pharmacologic treatment at the moment of blood collection. It consists of a total of 17,092 images and is organized into 8 classes (basophil, eosinophil, erythroblast, immature granulocytes (myelocytes, metamyelocytes and promyelocytes), lymphocyte, monocyte, neutrophil, platelet).

For this dataset, we first extract concepts for the 8 blood cell types via GPT using the following prompt, “*What are the features that can distinguish blood cell class name from rest of the blood cell types on their size, shape, nucleus appearance, and the presence of granules in their cytoplasm*”. We obtain 10 concepts for every blood cell type, for instance, for *platelets*, we get the following concepts, “*Smallest blood component*”, “*No nucleus*”, “*Granules present*”, “*Irregular shape*”, “*Cytoplasmic fragments*”, “*Variable granule distribution*”, “*Oval to round shape*”, “*Small dense granules*”, “*Lacks chromatin*”, “*Compact cytoplasmic body*”.

To test the coreset performance, we use a ResNet-18 model and report accuracy of our coresets in Table 11. Similar to other results, our method achieves better performance than randomly selected coresets for higher pruning rates and is competitive at lower pruning ratios. This is attributes to the difficulty of calculating concept similarity is the representation space of the CLIP model which is potentially unaware of the terminology used in the medical domain. While replacing CLIP with a VLM that is trained on medical domain can boost the performance of our method, our results highlight that even with access to such a model our approach is able to find better coresets than random subsets.

Our results on these two tasks highlight the versatility of our approach for model-agnostic approach to coreset selection, which is able to find coreset without requiring training the the downstream models on the entire dataset even once.

C.3 Evaluation on adaptive subset selection

In this section, we present a comparison of using our concept-based method for the problem of adaptive subset selection [30, 31, 71] (See App. A for a description of the problem). To test our approach, we followed the experimental setup of [71], of training a ResNet-18 model on CIFAR-10/100 for 300 epochs and changing the subset every 20 epochs. Unlike works in the line of adaptive subset selection which focus on selecting subsets that do not overlap or train models on easy subsets first before moving to difficult ones, we simply used our CCS-based selection approach [86] to

Table 13: Superior performance of downstream models with different architectures trained on our coresets for Imagenet compared to Random for both standard (Ours) and label-free (Ours-LF) CS highlight our transferability of our coresets.

Model Architecture	Method	Pruning Rates			
		30%	50%	70%	90%
MobileNet	Random	62.68 \pm 0.09	62.49 \pm 0.15	61.53 \pm 0.29	53.80 \pm 0.17
	Ours-LF	61.60 \pm 0.18	61.97 \pm 0.08	61.73 \pm 0.25	54.39 \pm 0.66
	Ours	61.36 \pm 0.15	62.32 \pm 0.22	62.46 \pm 0.26	55.57 \pm 0.13
RN-34	Random	73.37 \pm 0.08	71.71 \pm 0.10	67.85 \pm 0.04	51.29 \pm 0.20
	Ours-LF	73.61 \pm 0.08	71.99 \pm 0.05	68.42 \pm 0.21	53.52 \pm 0.06
	Ours	73.39 \pm 0.12	72.34 \pm 0.13	69.44 \pm 0.17	55.92 \pm 0.02
ViT-B-16	Random	59.09 \pm 0.49	51.65 \pm 0.46	40.19 \pm 0.13	22.13 \pm 0.16
	Ours-LF	57.50 \pm 0.69	49.81 \pm 0.89	40.33 \pm 0.86	23.08 \pm 0.27
	Ours	57.62 \pm 0.56	52.67 \pm 0.49	42.15 \pm 0.81	24.43 \pm 0.28

identify new subsets every 20 epochs for this task. Due to the randomness in CCS (Alg. 1), samples being selected to form the coreset changes.

In our table 12, we compare our method to previous methods and with an adaptive random selection method (where a random subset of data is selected every 20 epochs), which has been suggested by [31] as a strong baseline for this line of work. We observe that our method without any modifications achieves comparable performance to existing adaptive subset selection methods showing its effectiveness for this problem as well. Moreover, sampling new subsets via CCS (Alg. 1) is as efficient as sampling a random subset; thus our approach is also an efficient solution for this problem. While we believe that incorporating better subset sampling techniques as suggested by [31] may boost the performance of our method on this problem, CCS-based sampling is already quite effective.

C.4 Transferability of coresets

In this section, we present the performance of three additional downstream model architectures after training on the coresets found by our approach. Similar to the results in Table 3, our results in Table 13 show that coresets found by our approach in both standard and label-free setting achieve performance better than the random subsets on these three architectures as well. We note that the performance of the ViT model is worse than the performance of other model architectures with and without pruning (ViT-B-16 achieves an accuracy of $\approx 62\%$ compared to $\approx 78\%$ with ResNet-50 on full Imagenet dataset) due to the ViT models being data hungry in nature [14] and the fact that we used standard SGD-based training (similar to that used for training other models in the paper). We believe that using other training methods for ViTs as suggested in [69] could produce better performing ViT models.

Nonetheless, better performance than random subsets across a variety of downstream model architectures highlights the effectiveness of our approach at finding coresets without the knowledge of the architecture or training dynamics of the downstream models.

C.5 Algorithm for stratified sampling using CCS [86]

Here we present the algorithm for sampling the training examples to form the coreset based on the coverage-based selection methodology proposed by [86]. A crucial component of the algorithm is the cutoff rate β which controls how many challenging samples should be removed from consideration when selecting the coreset. This is done to eliminate misclassified samples from the dataset since they can hurt the performance of the model trained on coreset, especially at high pruning rates. Previous works [86, 87] ablate the values of this cutoff ratio by training the downstream model on a range of values. In our work, we simply use the values proposed by the previous works and find that they work well for our score as well. The cutoff rates β for different pruning rates α are as follows (α, β) . For CIFAR-10: (30%, 0), (50%, 0), (70%, 10%), (90%, 30%), for CIFAR-100: (30%, 10%), (50%, 20%), (70%, 20%), (90%, 50%), for Imagenet: (30%, 0), (50%, 10%), (70%, 20%), (90%, 30%). We used CCS for label-free CS as well and the cutoff rates used were for CIFAR-10: (30%, 0), (50%, 0), (70%, 20%), (90%, 40%), for CIFAR-100: (30%, 0), (50%, 20%), (70%, 40%), (90%, 50%), for Imagenet: (30%, 0), (50%, 10%), (70%, 20%), (90%, 30%).

Algorithm 1 Coverage-centric Coreset Selection (CCS) [86]

Input: Dataset with difficulty scores: $\mathbb{D} = \{(x, y, s)\}_{i=1}^n$, pruning ratio: α , cutoff rate: β , number of bins: b .

Output: Coreset: \mathcal{S}

```
# Prune hardest examples
 $\mathbb{D}' \leftarrow \mathbb{D} \setminus \{\lfloor n \times \beta \rfloor \text{ hardest examples}\}$ 
 $A_1, A_2, \dots, A_b \leftarrow \text{Split scores in } \mathbb{D}' \text{ into } b \text{ bins.}$ 
 $\mathcal{B} \leftarrow \{B_i : B_i \text{ consists of samples with scores in } A_i \text{ for } i = 1, \dots, b\}.$ 
# Define the size of the coreset
 $m \leftarrow n \times \alpha.$ 
```

```
while  $\mathcal{B} \neq \emptyset$  do
  # Select the bin with the fewest examples
   $B_{min} \leftarrow \arg \min_{B \in \mathcal{B}} |B|.$ 
  # Compute the budgets for this bin
   $m_B \leftarrow \min\{|B|, \lfloor \frac{m}{|\mathcal{B}|} \rfloor\}.$ 
   $\mathcal{S}_B \leftarrow \text{randomly sample } m_B \text{ samples from } B_{min}.$ 
   $\mathcal{C} \leftarrow \mathcal{C} \cup \mathcal{S}_B.$ 
   $\mathcal{B} \leftarrow \mathcal{B} \setminus \{B_{min}\}.$ 
   $m \leftarrow m - m_B.$ 
end while
return  $\mathcal{C}.$ 
```

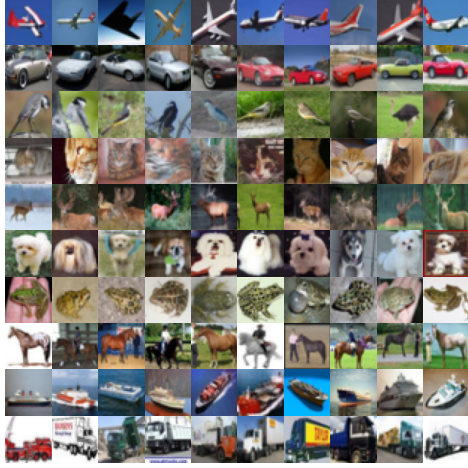
C.6 Experimental details

For generating the importance score we pre-compute the concept similarity scores for the entire dataset and then train the concept-bottleneck layer (in block 2 of Fig. 2) for 100 epochs across all experiments. This training only requires 800 seconds for Imagenet which is significantly more efficient than training the ResNet-34 model on Imagenet (requires roughly 8 hours on two A-100 GPUs). The accuracies of the models trained on the entire training set are 95.44% and 78.74% for ResNet(RN)-18 on CIFAR-10/100 and 72.4% for RN-18, 75% for RN-34, and 78.4% for RN-50 on Imagenet.

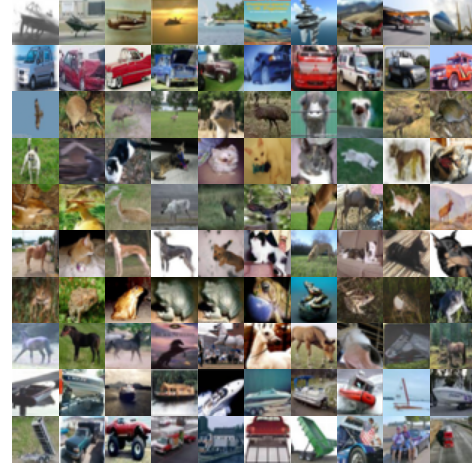
After the coresets are selected, we use the setting and code from [86] for training a ResNet-18 model for 40000 iterations with a batch size of 256 on the coresets for all pruning ratios for CIFAR-10/CIFAR-100. For Imagenet, we train ResNet-18, ResNet-34, and ResNet-50 models for 100 epochs on the coresets identified by our method using the training code based on FFCV [37].

The performance of the label-free CS is dependent on the quality of the pseudo-labels. Compared to the clustering-based approach used by ELFS [87], our approach of using the zero-shot classification ability of CLIP models yields significantly better pseudo-label quality along with being simpler and more efficient to compute. Specifically, for CIFAR-10/100, pseudo-labels of the training set are computed using the CLIP L-14 model trained on the DataComp-1B dataset [27] yields an accuracy of 98.52% and 87.28% whereas for Imagenet it achieves an accuracy of 79.47% which are better than the best pseudo-label accuracy obtained by the clustering approach in ELFS (92.5% and 66.3% on CIFAR-10/100 and 58.8% on Imagenet).

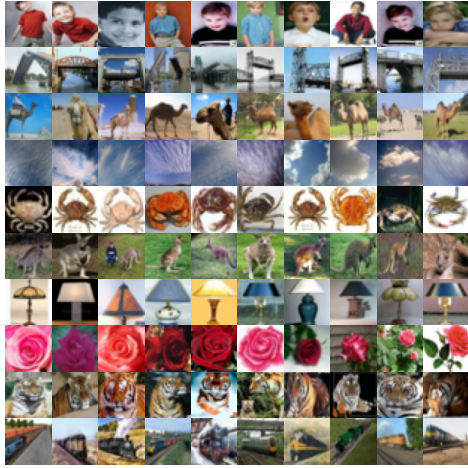
For training the concept bottleneck layer we minimized the cross entropy loss using SGD with a learning rate of 1E-3, momentum of 0.9 and a weight decay of 5E-4 for 100 epochs.



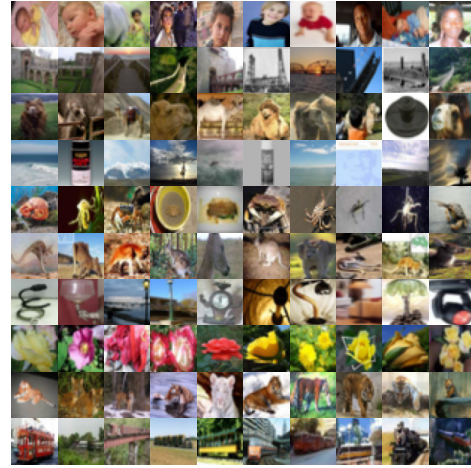
(a) Easy images from CIFAR-10



(b) Challenging images from CIFAR-10



(c) Easy images from CIFAR-100



(d) Challenging images from CIFAR-100

Figure 4: Class-wise easy and challenging images for the 10 classes (airplane, car, bird, cat, deer, dog, frog, horse, ship, truck) in CIFAR-10 and for a subset of 10 classes (boy, bridge, camel, cloud, crab, kangaroo, lamp, rose, tiger, train) from CIFAR-100. Similar to the results in Fig. 3, easy images (a,c) are more canonical images associated with the class labels whereas challenging images (b,d) are images that are confused between two or more classes in the dataset.